Proc. Natl. Acad. Sci. USA
Vol. 87, pp. 8408–8412, November 1990
Biophysics

Cytochrome *c* oxidase: Decay of the primary oxygen intermediate involves direct electron transfer from cytochrome *a*

SANGHWA HAN, YUAN-CHIN CHING, AND DENIS L. ROUSSEAU

AT&T Bell Laboratories, Murray Hill, NJ 07974

Communicated by Harry B. Gray, July 26, 1990

ABSTRACT **The decay of the primary intermediate generated in the reaction of oxygen with cytochrome *c* oxidase is nearly one order of magnitude faster in the fully reduced form of the enzyme than it is in the mixed valence form. To account for this observation, we propose a model describing the early molecular events in the reaction. In this model the decay of the primary Fe–O_2 intermediate in the fully reduced enzyme is a consequence of direct electron transfer from cytochrome *a*. To test the model we measured the time dependence of the oxidation of cytochrome *a* by monitoring the resonance Raman scattering intensity of its vibrational modes. A rapid oxidation of cytochrome *a* was detected that quantitatively agrees with the model. These results indicate that the mechanism of oxygen reduction and proposed frameworks for proton translocation must be reexamined.**

Cytochrome *c* oxidase catalyzes the four-electron reduction of dioxygen to water and translocates protons vectorially across the inner mitochondrial membrane. The redox active centers of the enzyme are the two heme groups, cytochrome *a* and cytochrome a_3, and two copper atoms, Cu_A and Cu_B. It is now well established that Cu_B and cytochrome a_3 form a binuclear site that binds dioxygen, and electrons from cytochrome *c* are transferred to the binuclear site via Cu_A and cytochrome *a* (1). The determination of the molecular basis for the mechanisms of the complex O_2 reduction and proton translocation requires knowledge of the structure and the kinetic properties of each of the reaction intermediates in the catalytic cycle. This information has been difficult to obtain at physiological temperatures because reliance has been made primarily on optical absorption spectra in which there is extensive overlap of absorption bands from each of the redox centers and the various intermediates (2–6).

Resonance Raman spectroscopy is a very powerful technique for probing the bound-ligand structure (7, 8, 31) and the redox states of the metal centers in cytochrome *c* oxidase (23) since isolated marker lines are present in the structure-rich spectra. To follow the formation and decay of the intermediates in the reaction of oxygen with cytochrome *c* oxidase, we have coupled resonance Raman scattering with the flow-flash-probe method (2) of synchronously initiating the oxygen reduction process (9–11). With this technique we have identified the Fe–O_2 stretching mode of the primary intermediate at 568 cm^{-1}, which is the same frequency as that in oxyhemoglobin and oxymyoglobin, suggesting that the molecular structure at the physiological binding site is not unique in cytochrome *c* oxidase (9, 11). By following the change in intensity of the Fe–O_2 stretching mode, the rate constants for the decay of the primary intermediate in the fully reduced (FR) (a^{2+} Cu_A^{1+}, a_3^{2+} Cu_B^{1+}) and in the mixed valence (MV) (a^{3+} Cu_A^{2+}, a_3^{2+} Cu_B^{1+}) forms of the enzyme were found (10, 11) to be 3.5×10^4 s^{-1} and 4.5×10^3 s^{-1}, respectively. Although the oxidation states of each of the redox centers during enzyme turnover under physiological conditions are not known, these two forms of the enzyme are useful models for determining the structures and properties of the catalytic intermediates.

In the past it has been assumed that the first step in the decay of the primary oxygen intermediate in the FR and the MV forms of the enzyme was electron transfer from the spectrally silent Cu_B to the Fe–O_2 complex of cytochrome a_3 (6, 12–15), although a branched mechanism with a pathway in which cytochrome *a* rather than Cu_B is rapidly oxidized has been proposed (3, 4). Based on the model that the primary oxygen intermediate in both the FR and MV forms of the enzyme decays by electron transfer from Cu_B, the difference between the rate of decay of the primary intermediate in these two forms of the enzyme was attributed to conformational changes at the binuclear site induced by the change in the redox state of the low-potential sites (Cu_A and cytochrome *a*). The existence and identity of such conformational changes during the O_2 reduction process in cytochrome *c* oxidase is a difficult matter to either prove or disprove since interactions between redox centers have been reported (16–20) but no definitive spectroscopic evidence has yet been observed. However, by considering that the iron–oxygen stretching frequency, which is sensitive to the structure of the Fe–O_2 complex, is the same in the FR and the MV forms of the enzyme (9, 11), the evidence becomes weaker that the active site undergoes a large conformational change upon reduction of the low-potential sites. Moreover, the vibrational properties of the CO ligand in carbon monoxide-bound cytochrome a_3 indicate that the dioxygen site is rigid and not subject to conformational modulation by the redox states of other centers (21). Therefore, it is difficult to rationalize the large difference in the rate constants if it is assumed that the decay is a consequence of electron transfer from Cu_B to the Fe–O_2 complex.

To determine the role played by cytochrome *a* in the reaction of oxygen with cytochrome *c* oxidase and its mechanism of influence on the rate of decay of the primary oxygen intermediate, we have measured the change in intensity of vibrational modes associated with either oxidized or reduced cytochrome *a*, as a function of time. By monitoring the intensities of these modes, the redox level of this center may be determined unambiguously. We find that cytochrome *a* becomes oxidized very rapidly. To account for this observation, we propose a model describing the early molecular events in the reaction of O_2 with fully reduced cytochrome *c* oxidase. In this model direct electron transfer from cytochrome *a* to the bound Fe–O_2 complex of the primary intermediate occurs. The model is supported by resonance Raman scattering data and their analyses that demonstrate that it is unnecessary to invoke any conformational change at the binuclear site to account for the kinetic data when redox states of the low-potential sites change. Instead, the data may be fully accounted for by the direct electron transfer mechanism that we propose. In view of these results, the mech-

The publication costs of this article were defrayed in part by page charge payment. This article must therefore be hereby marked "*advertisement*" in accordance with 18 U.S.C. §1734 solely to indicate this fact.

Abbreviations: FR, fully reduced; MV, mixed valence.

anism of oxygen reduction and possible frameworks for proton translocation must be reexamined.

EXPERIMENTAL METHODS

Cytochrome *c* oxidase was isolated from beef hearts according to the method of Yoshikawa *et al.* (22). The enzyme (200 μM) in 100 mM potassium phosphate (pH 7.4) containing 0.4% dodecyl β-D-maltoside was reduced anaerobically in the presence of 20 mM ascorbate and 3 μM cytochrome *c*. Carbon monoxide was introduced to the FR enzyme to prepare the CO complex. At each step the integrity of the enzyme was confirmed by obtaining the optical absorption spectrum on a UV-VIS spectrometer (SLM Aminco, Urbana, IL).

To generate the intermediates in the reaction of O_2 with cytochrome *c* oxidase, a syringe was filled with the CO-bound form of the reduced enzyme and another syringe was filled with buffer [100 mM potassium phosphate (pH 7.4)] saturated with O_2. The solutions were mixed in a Wiskind four-grid mixer (Update Instruments, Madison, WI) and then flowed into a Raman scattering cell. This quartz cell is 2 cm long and has an inner cross section of 0.25 × 0.25 mm. Two laser beams were directed onto the cell. The first at 413.1 nm, focused with a cylindrical lens, photodissociated the CO initiating the reaction of the enzyme with O_2. The second beam (either 413.1 or 441.6 nm), which could be moved with respect to the first, probed the Raman spectrum. The focal area of the laser beams and the flow rate of the mixed enzyme solution was set such that the sample passed through each of the laser beams areas in 15 μs. The sample was flowed continuously for the duration of each measurement. The separation between the photolysis and the probe laser beams could be adjusted to give a time delay ranging from 0 to 200 μs.

The scattered light from the probe beam was dispersed with a 1.25-m spectrograph (Spex Industries, Metuchen, NJ) and detected with a linear photodiode array (Princeton Applied Research). The pixel-to-pixel variation in the sensitivity of the detector was corrected by dividing the experimental spectrum by the spectrum of a white light source. No other corrections were done. Typical accumulation time for each spectrum was 30 s and the spectral solution was about 5 cm^{-1}.

RESULTS AND DISCUSSION

Representative data obtained at various time intervals after photolysis of CO and subsequent reaction of the enzyme with O_2 are shown in Fig. 1. Several lines may be assigned (23) to either oxidized or reduced cytochrome *a*. Among the most prominent are the lines at 1519, 1611, and 1649 cm^{-1}. The former two lines originate from reduced cytochrome *a* and the latter from the oxidized form of this center. The top spectrum in Fig. 1 is that of the FR enzyme in the absence of ligands, obtained by photolyzing the CO-bound enzyme anaerobically. The progress of the reaction of the enzyme with oxygen is followed from spectra B through F as a function of time. The time delay is determined by the flow rate, the size of the sample cell, and the physical separation between the photolysis and probe beams (413.1 nm). It is evident from the data that, even for the shortest probe-photolysis delay-time, oxidation of cytochrome *a* has already started to occur. Inspection of the data indicates that over the time course of the experiments reported here cytochrome *a* has been significantly oxidized. With a different excitation wavelength for the probe beam, 441.6 nm, which selectively enhances only reduced cytochrome *a* (24, 25), equivalent results were obtained.

To account for the rapid partial oxidation of cytochrome *a*, we propose a very simple model (Fig. 2) for the early steps

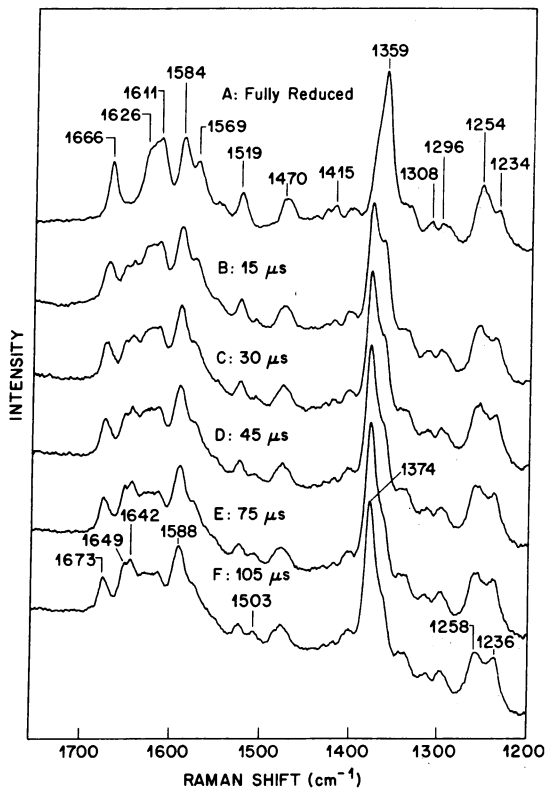

FIG. 1. Time dependence of the reaction of cytochrome *c* oxidase with oxygen. Spectrum A is from the carbon monoxide-bound enzyme photodissociated anaerobically to yield the FR form. Spectra B–F are from the enzyme photodissociated in the presence of oxygen. Each spectrum follows the time evolution of the changes in the hemes. The lines at 1519, 1611, and 1626 cm^{-1} are markers of reduced cytochrome *a* and the line at 1649 cm^{-1} is a marker of oxidized cytochrome *a*. The wavelength of both the probe and photolysis beams was 413.1 nm. The accumulation time for each spectrum was 30 s and the spectral resolution on the array detector was ≈5 cm^{-1}.

in the oxygen reduction process. In this scheme all of the rate constants are determined experimentally. The key elements of this model are as follows. (*i*) Reduction of the low-potential sites (cytochrome *a* and Cu_A) induces no conformational change to affect the electron transfer rate from Cu_B to the bound Fe–O_2 complex. Thus, k_2, the rate of electron transfer from Cu_B to the bound Fe–O_2 complex, which is the experimentally (10) determined rate of decay of the primary intermediate in the MV enzyme (4.5×10^3 s^{-1}), is the same regardless of the redox state of the low-potential sites. (*ii*) In FR cytochrome *c* oxidase, electron transfer takes place directly from cytochrome *a* to the oxygen-bound binuclear site. The rate constant for this process ($k_3 = 3 \times 10^4$ s^{-1}) was determined by subtracting the rate constant (4.5×10^3 s^{-1}) for the electron transfer from Cu_B to the Fe–O_2 complex measured in the MV experiments (10) from the measured decay rate (3.5×10^4 s^{-1}) of the primary intermediate in the FR enzyme (11). (*iii*) There is a rapid redox equilibrium between cytochrome *a* and Cu_A for which we adopt the reported values (26) for the forward (k_4) and reverse (k_{-4}) rate constants. The time dependence of the populations of the intermediates based on this model are presented in Fig. 3.

In the model the oxidation state of the Fe–O_2 complex is considered as a single unit. It was written this way because the degree of electron transfer to the bound oxygen in the primary intermediate is uncertain. We have considered (10) this question in a study of the oxygenation process in the MV form of the enzyme and found that the primary intermediate is most appropriately described as a superoxide complex;

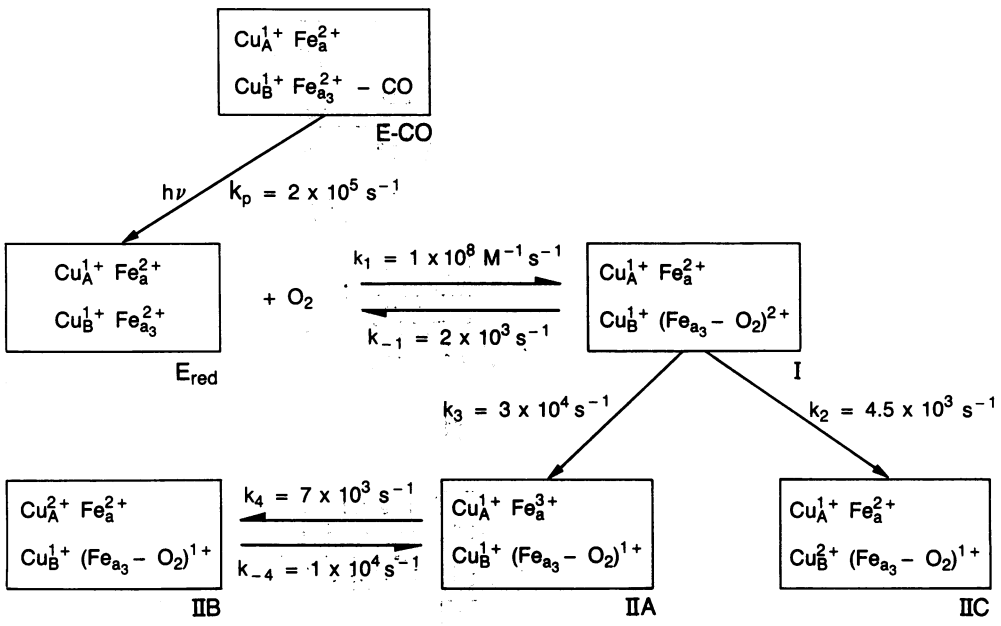

FIG. 2. Model for the early molecular events in the reaction of cytochrome *c* oxidase with oxygen. All of the rate constants were determined experimentally by us and others: an empirical constant to account for the photolysis of CO from the enzyme (k_p) was measured in anaerobic photolysis experiments; k_1 and k_{-1} are the reported forward and reverse rate constants for oxygen binding to the reduced binuclear center (3); k_2 was determined by measuring the decay of the primary intermediate in the MV enzyme (10); k_3 was obtained by subtracting k_2 from the decay of the primary intermediate in the FR enzyme (11); and k_4 and k_{-4} are the reported values for the equilibrium between the low-potential centers (26). The Fe–O_2 complex is written as having an oxidation state of 2+ when it displays properties similar to those of oxyhemoglobin or oxymyoglobin and 1+ when it has accepted one electron from another redox center.

i.e., upon binding dioxygen, an electron from cytochrome a_3 is transferred to it immediately. Therefore, in the model the three secondary intermediates (IIA, B, and C) are peroxide forms of the enzyme (two-electron reduced). In each of these intermediates the first electron originated from the cytochrome a_3 heme group. In IIA and IIB, the binuclear site is the same—i.e., a heme peroxide with Cu_B in its cuprous state. These two intermediates differ only in the formal assignment of the low-potential redox states. In IIA, Cu_A has lost an electron whereas, in II_B, cytochrome *a* has lost an electron. Intermediate IIC is a peroxide form of the enzyme in which the second electron originates from Cu_B. Thus, in our model peroxy states remain as obligatory intermediates in the oxygen reduction process. In this model the decay of intermediates IIA, B, and C are not considered since it is only a description of the early molecular events. Therefore, we do not address the origin of the changes reported at longer times.

To test this model, the time evolution of the oxidation of cytochrome *a* is compared to a computer calculation simulating our experimental conditions (Fig. 4). An alternative pathway, direct electron transfer from Cu_A to the Fe–O_2 complex, was also considered and the calculated oxidation of cytochrome *a* with this pathway is shown as the dashed curve in Fig. 4. Our experimental observations cannot be accounted for by this latter pathway without making the Cu_A-to-cytochrome *a* electron transfer rate unreasonably high ($k >> 5 \times 10^4\ s^{-1}$) since it has been reported to become oxidized

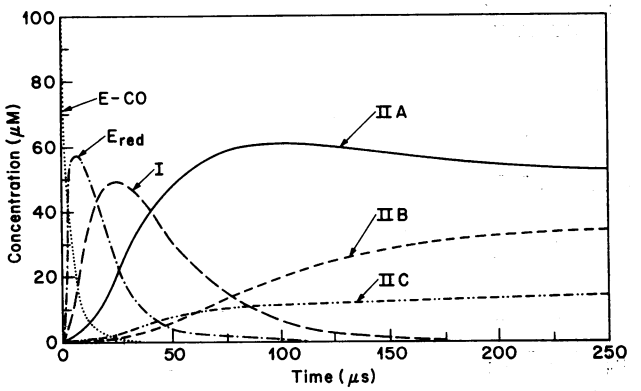

FIG. 3. Populations of each of the intermediates as a function of time, based on the scheme in Fig. 2. Further reactions of IIA, IIB, and IIC, which modify their populations at longer times, are not included in this scheme.

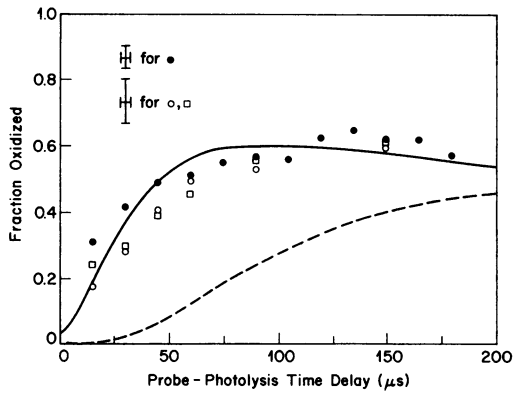

FIG. 4. Comparison between experimental measurements of the oxidation of cytochrome *a* and a computer simulation (solid line) under our experimental conditions. This calculation is based on the model described in Figs. 2 and 3 in which the decay of the primary intermediate involves direct electron transfer from cytochrome *a*. Data points for three marker lines are shown. The solid circles are from the line at 1519 cm^{-1} in reduced cytochrome *a* (413.1-nm excitation) and the open circles and squares are from the lines at 1626 and 1611 cm^{-1}, respectively, from reduced cytochrome *a* (441.6-nm excitation). The degree of oxidation was determined from a ratio of the intensity of each cytochrome *a* line in the spectrum of the intermediate to that in the spectrum of the ligand free FR enzyme. Estimated errors in the measurement of the time and intensity for each data set are indicated. The dashed line is a computer simulation of the oxidation of cytochrome *a* when the pathway for electron transfer to the Fe–O_2 complex is from Cu_A rather than cytochrome *a*.

with an apparent rate constant of 7×10^3 s^{-1} (3, 6). A model involving simultaneous electron transfer from both cytochrome *a* and Cu_A to the Fe–O_2 complex can not be excluded by our data but the rapid oxidation of cytochrome *a* and the reported (3, 6) lag in the oxidation of Cu_A ($k \approx 7 \times 10^3$ s^{-1}) argues against a large degree of direct electron transfer from Cu_A to the Fe–O_2 complex. We conclude that the experimental data is most consistent with the model we have presented in Figs. 2 and 3. Inclusion of direct electron transfer from Cu_A and optimization of the rate constants would lead to even better agreement between the data and the model. However, it was felt that the validity of the model was better tested by comparing the observed and calculated oxidation of cytochrome *a* without any adjustable parameters.

Intermediates in the reaction of oxygen with cytochrome *c* oxidase have also been studied at low temperature with the triple-trapping technique. In the original studies by Chance *et al.* (27, 28), the decay of the primary intermediate was interpreted as occurring by simultaneous oxidation of the heme in cytochrome a_3 and Cu_B, although some oxidation of cytochrome *a* and Cu_A was suggested by the optical and EPR spectra. Subsequent studies by Clore *et al.* (29) confirmed oxidation of cytochrome *a* or Cu_A in the first intermediate detected after the decay of the primary intermediate. Thus, direct electron transfer to the primary intermediate that we report here is also occurring at cryogenic temperatures. However, the relative kinetics of the formation of the various intermediates do not necessarily reflect those occurring at physiological temperatures. This possibility was recognized by Chance *et al.* (27) who pointed out that above −50°C electron transfer from cytochrome *a* could outstrip the conversion of the primary intermediate to compound B (Cu_A^{1+} a^{2+} Cu_B^{2+} a_3^{3+} O_2^{2-}). Furthermore, that the relative rates of the early molecular events are different at low temperature is indicated by the observation that the primary intermediate in the MV and the FR forms of the enzyme decay on the same time scale at 173 K (29, 30).

The model presented here is consistent with a large body of experimental observations. (*i*) It accounts quantitatively for the difference in the decay of the primary intermediate between the FR and the MV forms of the enzyme (4, 6, 9–11, 23). (*ii*) It confirms prior conclusions based on both low temperature (29) and room temperature experiments (3, 4) that cytochrome *a* rather than Cu_B becomes partially oxidized as the population of the primary intermediate decays. (*iii*) The model explains why the intermediate formed in the reaction of oxygen with the MV enzyme was not detected in the reaction of oxygen with the FR enzyme (5). (*iv*) It incorporates the reported (26) redox equilibrium between cytochrome *a* and Cu_A into the catalytic mechanism. (*v*) It accounts for the lag time in the oxidation of Cu_A with respect to the decay of the primary intermediate (3, 6).

Finally, we must ask if it is possible to account for the rapid oxidation of cytochrome *a* if the electron transfer from cytochrome *a* to the binuclear site follows the electron transfer from Cu_B to the Fe–O_2 complex, the generally accepted pathway. First, it is necessary to assume that the reduction of the low-potential sites (Cu_A and cytochrome *a*) gives rise to a conformational change that leads to nearly an order of magnitude faster electron transfer from Cu_B to the Fe–O_2 complex in the FR as compared to the MV form of the enzyme. Such a change cannot be ruled out since interactions between the redox centers have been detected. For example, conformational changes affecting the binding rate of ligands to the ferric state of cytochrome a_3 have been observed (16, 17). In addition, some changes in the optical properties (18) of cytochrome a_3 and changes in the redox potential (19, 20) of Cu_B, upon changing the redox states of the low-potential sites, have been reported. However, the effect of these changes on the rate of electron transfer from Cu_B to the Fe–O_2 complex has not been assessed quantitatively. Our model and our data do not rule out the possibility that the two electron-reduced intermediates (IIA and IIB) decay rapidly by the transfer of a third electron (from Cu_B) to the oxygenated complex forming three electron-reduced intermediates. The rate of formation of such intermediates will be determined when clear markers for them are identified. Relaxation of intermediate IIC will be difficult to determine since it accounts for only about 10% of the enzyme.

The data presented here and the time dependence of the early molecular events underscore the complexity of the oxygen reduction process. Our findings and the associated model show that the oxidation of all of the metal redox sites contribute to the decay of the primary intermediate simultaneously. Thus, to obtain a quantitative understanding of the O_2 reduction mechanism all redox centers should be monitored. Moreover, it is apparent that the generally accepted model of a sequential mechanism in which the Fe–O_2 complex decays primarily by electron transfer from Cu_B at physiological temperatures (6, 14, 15) must be reevaluated. A quantitative model of the initial electron transfer steps reported here and the determination of the later steps will lead to a better understanding of the structure of the catalytic intermediates and a framework on which to build concepts for proton translocation.

We thank Dr. G. Blondin of Water Resources Center for mitochondria. S.H. is partially supported by Grant GM-39359 from the National Institute of General Medical Sciences.

1. Wikström, M., Krab, K. & Saraste, M. (1981) *Cytochrome Oxidase: A Synthesis*, (Academic, New York).
2. Gibson, Q. & Greenwood, C. (1963) *Biochem. J.* **86**, 541–554.
3. Hill, B. C. & Greenwood, C. (1984) *Biochem. J.* **218**, 913–921.
4. Hill, B. C., Greenwood, C. & Nicholls, P. (1986) *Biochim. Biophys. Acta* **853**, 91–113.
5. Orii, Y. (1988) *Ann. N.Y. Acad. Sci.* **550**, 105–117.
6. Oliveberg, M., Brzezinski, P. & Malmström, B. G. (1989) *Biochim. Biophys. Acta* **977**, 322–328.
7. Argade, P. V., Ching, Y.-c. & Rousseau, D. L. (1984) *Science* **225**, 329–331.
8. Varotsis, C., Woodruff, W. H. & Babcock, G. T. (1989) *J. Am. Chem. Soc.* **111**, 6439–6440.
9. Han, S., Ching, Y.-c. & Rousseau, D. L. (1990) *Biochemistry* **29**, 1380–1384.
10. Han, S., Ching, Y.-c. & Rousseau, D. L. (1990) *J. Am. Chem. Soc.*, in press.
11. Han, S., Ching, Y.-c. & Rousseau, D. L. (1990) *Proc. Natl. Acad. Sci. USA* **87**, 2491–2495.
12. Wikström, M. (1987) *Chem. Scr.* **27B**, 53–58.
13. Orii, Y. (1988) *Chem. Scr.* **28A**, 63–69.
14. Wikström, M. (1989) *Nature (London)* **338**, 776–778.
15. Chan, S. I. & Li, P. M. (1990) *Biochemistry* **29**, 1–12.
16. Jones, M. G., Bickar, D., Wilson, M. T., Brunori, M., Colosimo, A. & Sarti, P. (1984) *Biochem. J.* **220**, 57–66.
17. Jensen, P., Wilson, M. T., Aasa, R. & Malmström, B. G. (1984) *Biochem. J.* **224**, 829–837.
18. Blair, D. F., Bocian, D. F., Babcock, G. T. & Chan, S. I. (1982) *Biochemistry* **21**, 6928–6935.
19. Blair, D. F., Ellis, W. R., Jr., Wang, H., Gray, H. B. & Chen, S. I. (1986) *J. Biol. Chem.* **261**, 11524–11537.
20. Goodman, G. (1984) *J. Biol. Chem.* **259**, 15094–15099.
21. Einarsdottir, O., Choc, M. G., Weldon, S. & Caughey, W. S. (1988) *J. Biol. Chem.* **263**, 13641–13654.
22. Yoshikawa, S., Choc, M. G., O'Toole, M. C. & Caughey, W. S. (1977) *J. Biol. Chem.* **252**, 5498–5508.
23. Babcock, G. T. (1988) in *Biological Applications of Raman Spectroscopy*, ed. Spiro, T. G. (Wiley, New York), Vol. 3, pp. 293–346.
24. Ching, Y.-c., Argade, P. V. & Rousseau, D. L. (1985) *Biochemistry* **24**, 4938–4946.
25. Argade, P. V., Ching, Y.-c. & Rousseau, D. L. (1986) *Biophys. J.* **50**, 613–620.

26. Morgan, J. E., Li, P. M., Jang, D.-J., El-Sayed, M. A. & Chan, S. I. (1989) *Biochemistry* **28,** 6975–6983.
27. Chance, B., Saronio, C. & Leigh, J. S., Jr. (1975) *J. Biol. Chem.* **250,** 9226–9237.
28. Chance, B., Saronio, C. & Leigh, J. S., Jr. (1975) *Proc. Natl. Acad. Sci. USA* **72,** 1635–1640.
29. Clore, G. M., Andreasson, L.-E., Karlsson, B., Aasa, R. & Malmström, B. G. (1980) *Biochem. J.* **185,** 139–154.
30. Clore, G. M., Andreasson, L.-E., Karlsson, B., Aasa, R. & Malmström, B. G. (1980) *Biochem. J.* **185,** 155–167.
31. Varotsis, C., Woodruff, W. H. & Babcock, G. T. (1989) *J. Am. Chem. Soc.* **112,** 1297.